An impaired hepatic clock system effects lipid metabolism in rats with nephropathy

PEIPEI CHEN[1], RUIYU ZHANG[1,2], LIJUN MOU[1,3], XUEWANG LI[1], YAN QIN[1] and XUEMEI LI[1]

[1]Department of Nephrology, Peking Union Medical College Hospital, Chinese Academy of Medical Sciences and Peking Union Medical College, Beijing 100730; [2]Department of Nephrology, Capital Medical University Affiliated with Beijing Anzhen Hospital, Beijing 100029; [3]Department of Nephrology, The Second Affiliated Hospital, School of Medicine Zhejiang University, Hangzhou, Zhejiang 310009, P.R. China

Received April 2, 2018; Accepted August 20, 2018

DOI: 10.3892/ijmm.2018.3833

Abstract. Hyperlipidemia is a key clinical feature in patients with nephrotic syndrome (NS) that is associated with the incidence of cardiovascular events. Recent studies have suggested that the disorders of triglycerides, gluconeogenesis and liver glucose metabolism are associated with the abnormal transcription of clock genes. However, changes to the circadian rhythm of blood lipids in NS require further exploration, and the effects of NS on the hepatic clock system remain to be elucidated. In the present study, the impaired diurnal rhythm of the hepatic core clock genes (*BMAL1*, *CLOCK*, *CRY1*, *CRY2*, *PER1* and *PER2*) significantly induced circadian rhythm abnormalities in liver-specific clock-controlled genes (*LXR, CYP7A1, SREBP-1, ABCA1, DEC1* and *DEC2*; all $P<0.05$), which were significantly associated with the abnormal diurnal rhythms of triglyceride, total cholesterol, aspartate aminotransferase and alanine aminotransferase (all $P<0.05$) in rats with Adriamycin-induced nephropathy. Furthermore, a protein-protein interaction network was identified. Gene Ontology and Kyoto Encyclopedia of Genes and Genomes pathway analyses based on the human database was conducted to obtain signaling pathway and correlation prediction analyses of overall human clock and clock-controlled gene correlations. Strong correlations of the aforementioned clock genes were detected (avg. local clustering coefficient, 0.849) which suggested significant enrichment in circadian rhythm signaling. The present results indicated that damage to hepatic clock systems may impact blood lipid circadian rhythm disorders in NS, and offer a starting point for understanding the crosstalk between peripheral organs and peripheral clock systems.

Correspondence to: Dr Yan Qin, Department of Nephrology, Peking Union Medical College Hospital, Chinese Academy of Medical Sciences and Peking Union Medical College, 1 Shuaifuyuan, Beijing 100730, P.R. China
E-mail: qinyanbeijing@126.com

Key words: nephrotic syndrome, circadian rhythm, clock-controlled genes, blood lipid, bioinformatics

Introduction

Patients with chronic kidney disease (CKD) exhibit major proatherogenic lipid abnormalities that are associated with their prognosis (1). The severe disorder of lipoprotein metabolism in patients with CKD typically manifests as higher triglyceride (TG) levels and lower levels of high-density lipoprotein cholesterol (HDL-C) (1). Dyslipidemia also increases the incidence of coronary atherosclerosis and cardiovascular events. Notably, improving hyperlipidemia may reduce dialysis morbidity and mortality in patients with end-stage renal disease.

Notably, the mechanisms of dyslipidemia in nephrotic syndrome (NS) are associated with hepatic biology, including liver lipid regulatory enzymes, activity of low-density lipoprotein (LDL) receptors and compensatory synthesis in the liver (2). Liver-associated physiological processes exhibit rhythmicity, and the circadian rhythm activities are regulated by central and hepatic-specific clock systems (3).

Diurnal oscillations are regulated by conserved clock genes in the organism, which act as a hierarchical, collaborative, large-scale 'circadian time' (4). The majority of biological processes, including the maintenance of blood pressure, sleeping and respiratory rhythm, exhibit circadian rhythmicity, and are also regulated by clock genes (5). These genes are expressed in all cell types, including the 'master clock' located in the suprachiasmatic nucleus and the peripheral clock in locations, such as the kidney and liver (4). A previous study indicated that genomic transcription was highly rhythmic, with ≤81.7% of protein-coding genes exhibiting daily rhythms in expression (6). These oscillators dominate the rhythmic expression of downstream clock-regulated genes, accounting for 10-15% of the genes that regulate the circadian characteristics of the physiological functions of peripheral organs (7).

The cell-autonomous molecular clock in mammals is generated by two interlocking transcription/translation feedback loops (TTFLs) that cooperate to produce robust rhythms of gene expression. The core TTFL is driven by two activators, circadian locomoter output cycles kaput (*CLOCK*) and brain and muscle ARNT-like protein 1 (*BMAL1*), and two repressors cryptochrome (*CRY*) and period homologue (*PER*) (8), which aid the organism to drive circadian rhythms of behavioral activity and hormones (9). Previous studies have

confirmed that the hepatic clock maintains normal glucose (GLU) levels, fatty acids, fat mobilization and the rhythm of other biochemical reactions in a steady state through the liver X receptor (LXR), peroxisome proliferator-activated receptor (PPAR) γ coactivator and PPAR signaling pathways to regulate TG, cholesterol and fat metabolism under physiological conditions (3,10).

The clock system serves an essential role in homeostasis. Notably, dyslipidemia is considered a homeostasis disorder event in NS. However, the effects of the circadian rhythmicity on blood lipids and the hepatic clock system in this context are unclear. Therefore, the present study was performed to observe the circadian rhythm of lipids and clock genes associated with lipid metabolism in Adriamycin (ADR)-induced nephropathy in rats to explore the potential effects of the clock system on lipid metabolism abnormalities.

Materials and methods

Experimental animals and treatment protocol. A total of 36 adult male Sprague Dawley rats (8-weeks old; 245-265 g) were purchased from Beijing HFK Bioscience Co., Ltd. (Beijing, China). The animal experimental procedures were approved by the Animal Ethics Committee of Peking Union Medical College Hospital (PUMCH; Beijing, China). Furthermore, all experiments were performed according to international and institutional guidelines for animal care (11), and approved by the PUMC Committee on Animal Care and Use. All rats had access to standard food and tap water *ad libitum*. Rats were housed at 23±2˚C (12,13), under a strict 12-h light/dark regimen whereby zeitgeber time ZT0-ZT12 with the lights on represented the resting phase of the day and ZT12-ZT0 with the lights off represented the active phase of the day. Following 2 weeks of adaptation, rats were randomly divided into two groups: ADR group (ADR-induced nephropathy rats) and control group (saline-treated rats). The NS model was established 14 days from the single intravenous tail injection of 6.5 mg/kg ADR (dissolved in saline; Pfizer, Inc., New York, NY, USA) according to the protocol by Bertani *et al* (14). Rats in the control group were injected with an equal volume of saline only. The experimental animals were fasted in a metabolic cage to assess 24-h urine excretion. A 24-h urine excretion value of >100 mg (15) and foot process effacement of renal tissues detected by electron microscopy (16) indicated the successful establishment of the NS model. After 2 weeks, the rats from the two groups were sampled every 4 h over 24 h (3 rats/group at each time point, with a total of 18 normal rats and 18 NS rats). During the sacrificed day, standard food and water was provided *ad libitum* and treatments were quickly finished to minimize the impact on the timer giver and animal, consistent with other literature methodologies (12,13). The handling of rats during the dark time period was performed under a dim red light, which does not influence endogenous melatonin production (17).

Blood samples and liver tissue. Rats from each group were sacrificed at ZT 2:00, 6:00, 10:00, 14:00, 18:00 and 22:00 h. The liver tissues were immediately frozen in liquid nitrogen and stored in RNAlater (cat. no. AM7020; Ambion; Thermo Fisher Scientific, Inc., Waltham, MA, USA) at -80˚C. Blood samples were centrifuged at 6,391 x g for 10 min at 4˚C. Samples were sent to the Department of Laboratory Medicine, PUMCH (Beijing, China). The following measurements were performed with a Hitachi Modular P800 analyzer (Hitachi, Ltd., Tokyo, Japan): Serum total cholesterol (TC) (CHOD-PAP method; Roche Diagnostics GmbH, Mannheim, Germany) (18), serum TGs (GP0-PAP method; Roche Diagnostics GmbH), and HDL-C (Roche HDL-C Plus 2nd generation kit; Roche Diagnostics GmbH). LDL-C was calculated using the Friedewald formula (19). Albumin was measured using the bromo-potassium phenol green method (20) and serum creatinine was measured using a sarcosine oxidase method (21). Aspartate aminotransferase (AST) and alanine aminotransferase (ALT) activity was assessed with an automatic biochemical analyzer. Furthermore, GLU levels were measured using the hexokinase method (22).

Transmission electron microscopy analyses. Fresh rat renal tissues were removed in sections of ~2.0 mm^3 and fixed with 2.5% glutaraldehyde in 0.1 M Sorenson's phosphate buffer (pH=7.41) for 2 h at 4˚C. Following this, the samples were washed three times with 0.1 M Sorenson's phosphate buffer. The tissues were subsequently post-fixed for 1-1.5 h in 1% OsO_4 in 0.1 M Sorenson's phosphate buffer, washed with distilled water, then stained *en bloc* with 3% uranyl acetate for 30 min at 25˚C. Dehydration was performed using a 50-95% graded ethanol series, followed by two changes in propylene oxide. Sections of 70-80 nm were cut, and collected on a 200 copper/rhodium grid stained with uranyl acetate and lead citrate. Following this, samples were observed under a transmission electron microscope (magnification, x5,000).

Reverse transcription-quantitative polymerase chain reaction (RT-qPCR) analysis. Total RNA was extracted from frozen heart tissues using RNAiso Plus reagents (cat. no. 9109; Takara Bio, Inc., Otsu, Japan) according to the manufacturer's protocol. RNA was reverse transcribed using the PrimeScript® RT Master Perfect Real-time kit (cat. no. DRR036A; Takara Bio, Inc.). The resulting cDNA was amplified using a SYBR-Green PCR kit (cat. no. DRR082A; Takara Bio, Inc.) and detected with a 7500 Fast Real-time PCR system (Applied Biosystems; Thermo Fisher Scientific, Inc.). All experiments were performed at least three times according to the manufacturer's protocol. The conditions for the two-step amplification PCR reaction were pre-denaturation (95˚C, 30 sec, 1 cycle) and PCR amplification (95˚C, 5 sec and 60˚C, 30 sec, 40 cycles). Gene expression was calculated relative to the housekeeping gene *GAPDH* using the $2^{-\Delta\Delta Cq}$ method (23). The primers used for PCR are presented in Table I.

Protein-protein interaction (PPI) network and functional enrichment of protein-coding genes. Due to the difficulties of obtaining human tissues to explore the rhythmic characteristics of clock gene expression levels every 4 h, correlation analyses of the expression levels of human proteins were performed using the STRING database (http://www.string-db.org/) (24) as a complementary platform to assessed the association between core clock and clock-controlled genes in patients with renal disease. Furthermore, the DAVID Bioinformatics Tool (25) was used to identify functional enrichment of target

Table I. Primers for reverse transcription-quantitative polymerase chain reaction.

Gene	Forward (5'-3')	Reverse (5'-3')
GAPDH	GACAACTTTGGCATCGTGGA	ATGCAGGGATGATGTTCTGG
CLOCK	CATCGGCAGCAAGAAGAACT	CAAGATTCAGTCCAGGGTTTG
BMAL1	CAACCCATACACAGAAGCAAAC	ACAGATTCGGAGACAAAGAGGA
PER1	GAGGAGCCAGAGAGGAAAGAGT	TTGGTTGTGTTAGGAATGTTGC
PER2	CTGGAAAGAACAGGAAACTGAA	GGGAACACAGGTAGTGGGTAAG
CRY1	ATCTAGCCCGACATGCAGTT	TCGGCGTCAAGCAGTAATTC
CRY2	ATTGAGCGGATGAAGCAGAT	TCTACACAGGAAGGGACAGATG
LXR	CCTGATGTTTCTCCTGACTC	TGACTCCAACCCTATCCTTA
DEC1	CCACCAAAAAGAGCCGAAT	ATAGAAGGGCAGGCAAAAGG
DEC2	GAAGCGAGACGACACCAAG	TTTCAGATGTTCAGGCAGTAAGTC
SREBP-1	GGAGCCATGGATTGCACATT	GGCCCGGGAAGTCACTGT
ABCA1	CTTGCTTCCGTTATCCAACTCCAG	GCTGTAATGTTCTCAGGACCTTGTG
CYP7A1	CCAAGTCAAGTGTCCCCCTCTA	GACTCTCAGCCGCCAAGTG

CLOCK, circadian locomoter output cycles kaput; *BMAL1*, brain and muscle ARNT-like protein 1; *CRY*, cryptochrome; *PER*, period homologue; *LXR*, liver X receptor; *CYP7A1*, cholesterol 7α-hydroxylase; *SREBP-1*, sterol regulatory element binding protein-1c; *ABCA1*, ATP binding cassette transporter A1; *DEC*, differentiated embryo chondrocyte.

protein-coding genes. Notably, this tool may be used to identify Gene Ontology (GO) biological processes associated with protein-coding genes. Furthermore, KEGG pathway enrichment analysis was performed using KOBAS 3.0 (http://kobas.cbi.pku.edu.cn/). Cytoscape (www.cytoscape.org/) (26) was also used to visualize the above biological process organization and GOplot (http://wencke.github.io/) (27) was used to illustrate the functional analysis data.

Statistical analysis. The results are presented as the mean ± standard deviation, and the data were analyzed using unpaired t-tests with SPSS 20.0 software (IBM Corp., Armonk, NY, USA) for comparisons between groups. $P<0.05$ was considered to indicate a statistically significant difference. Gene expression data and blood parameters were analyzed to assess the circadian rhythmicity of data using a Fourier transform method and Chronos-Fit software (http://chronos-fit.software.informer.com/). Following the Chronos-Fit software formula: $F(t)=mesor+\Sigma$ (amplitude$_i$ x cos (t-acrophase$_i$) x 2π/pi). The parameters included the mean, midline estimating statistic of rhythm (mesor), amplitude of the sine wave (amplitude) and the acrophase or time of maximum of the sine wave (acrophase). The chart indicated the curve fitted to the circadian analysis of all clock genes. Significance ($P<0.05$) was evaluated using the F-test as described previously (28,29).

Results

Rats with nephropathy exhibit hyperglycemia and disordered rhythms in serum TC, TG, AST and ALT levels. The ADR-induced nephropathy model is a classical nephropathy animal model (16,30). In the present study, 2 weeks following ADR injection, the ADR group presented with minimal change in disease according to the electron microscopy results (Fig. 1). The levels of blood TC, TG, HDL-C, LDL cholesterol (LDL-C) and GLU over 24 h were significantly increased in the ADR group compared with the control group (all $P<0.05$, Table II). AST and ALT activity was also significantly increased in the ADR group compared with the control group

Table II. Laboratory parameters in the two groups.

Measure	SD rats (n=18)	ADR rats (n=18)	P-value
ALB (g/l)	29.78±2.13	22.14±2.75[a]	<0.05
SCr (μmol/l)	34.05±13.94	39.06±7.59	0.231
BUN (mmol/l)	7.01±1.34	7.00±1.50	0.968
TC (mmol/l)	1.80±0.29	4.45±1.47[a]	<0.05
TG (mmol/l)	0.71±0.56	3.97±2.87[a]	<0.05
HDL-C (mmol/l)	0.59±0.09	1.27±0.38[a]	<0.05
LDL-C (mmol/l)	0.25±0.05	0.68±0.23[a]	<0.05
GLU (mg/dl)	176.64±21.55	336.89±102.65[a]	<0.05
AST (U/l)	88.30±16.73	120.51±22.85[a]	<0.05
ALT (U/l)	51.73±10.66	70.59±15.30[a]	<0.05
24 h UP (mg/day)	21.70±7.53	178.30±68.53[a]	<0.05

[a]$P<0.05$ (between-group comparison). Values are expressed as the mean ± standard deviation. ALB, albumin; SCr, serum creatinine; BUN, blood urea nitrogen; TC, total cholesterol; TG, triglyceride; HDL-C, high-density lipoprotein cholesterol; LDL-C, low-density lipoprotein cholesterol; GLU, glucose; AST, Aspartate aminotransferase; ALT, Alanine aminotransferase; 24 h UP, urine protein; SD, Sprague-Dawley control rats; ADR, Adriamycin-induced nephropathy.

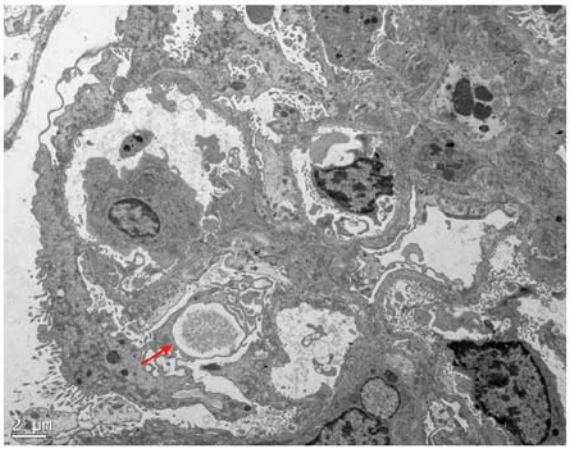

Figure 1. Electron microscopic observation of extensive foot process fusion in renal tissue of Adriamycin-induced nephropathy rats (red arrow).

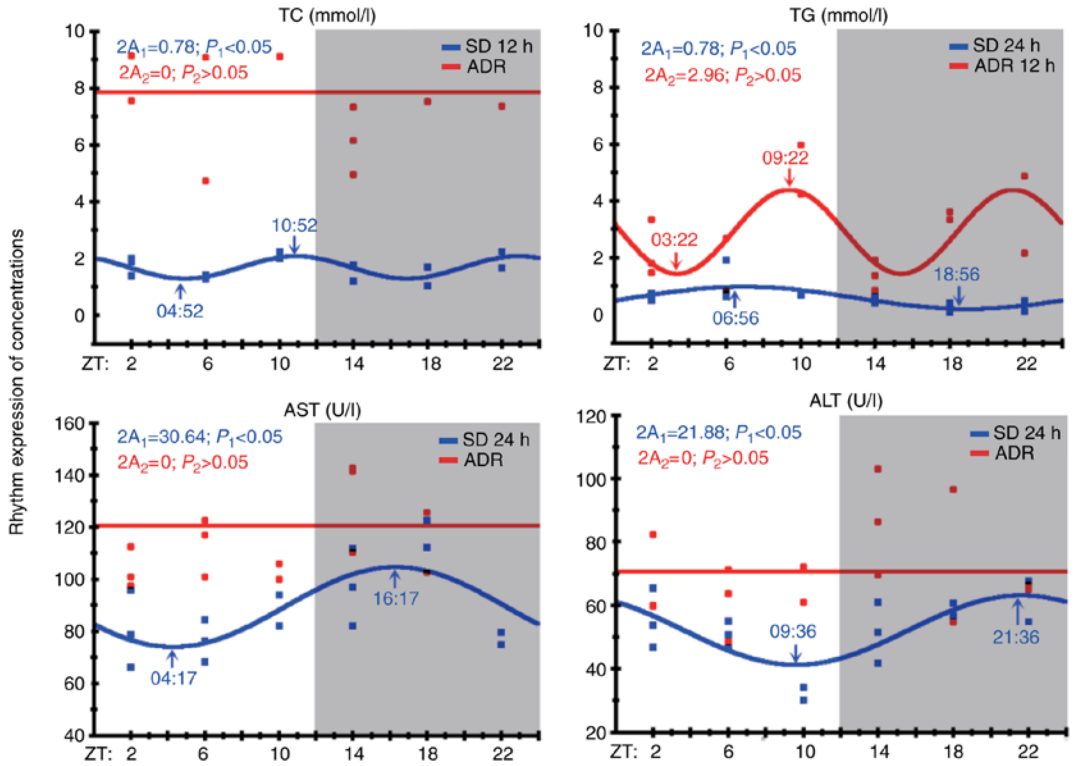

Figure 2. TC, TG, AST and ALT levels are associated with a circadian pattern. Arrows in each figure indicate the ZT was associated with the peak value and off-peak value of the fitted curve (acrophase). The chart shows the fitted curve generated by circadian analysis of all clock genes; this curve was checked for significance using the F-test (P<0.05). 2A1 is the double amplitude of the control group, and 2A2 is the double amplitude of the ADR group. Gray area, dark period (ZT=12:00-24:00); white area, light period (ZT=00:00-12:00). The blue and red dots indicate the measured TC, TG, AST and ALT levels in the control and ADR groups during the light and dark periods, respectively. Partial Fourier analysis, n=36, three rats/group every 4 h in 24 h. ADR, Adriamycin-induced nephropathy; TC, total cholesterol; TG, triglyceride; AST, aspartate aminotransferase; ALT, alanine aminotransferase; ZT, Zeitgeber time.

(P<0.05, Table II). In the control group, the serum levels of TC, TG, AST and ALT were significantly cycled every 12, 24, 24 or 24 h, respectively (all P<0.05), and the double amplitudes (2A) of the TC and TG levels were similar (2A=0.78). However, in the ADR group, the rhythm of the TG levels changed from the baseline of 24 to 12 h, and no oscillations were observed with regards to TC, AST and ALT levels (all P>0.05; Fig. 2). The HDL-C, LDL-C and GLU levels in the two groups did not indicate a circadian rhythm (F-test, P>0.05; data not shown).

Hepatic core clock and clock-controlled genes that regulate TG, cholesterol and fat metabolism are associated with disordered rhythms in NS rats. The circadian rhythm of six hepatic core clock genes and six clock-controlled genes associated with metabolism were evaluated. The data revealed the *CRY1* and *PER2* genes exhibited 24-h rhythmicity, and their peak times advanced by 0.5 and 2.5 h compared with those in the control group; however, the rhythm *of PER1* mRNA expression was wholly absent in the ADR group (P<0.05). Other core clock genes, including CLOCK and *CRY2*, exhibited a change in periodicity from 24 to 12 h, and their peak times significantly shifted to the rest period (daytime; P<0.05). Furthermore, the rhythm of *BMAL1* mRNA expression changed from 24 h to a period of 4.8+6 h (P<0.05; Fig. 3A).

The liver-specific clock-controlled genes, including *LXR*, cholesterol 7α-hydroxylase (*CYP7A1*), sterol regulatory element binding protein-1c (*SREBP-1*), ATP binding cassette transporter A1 (*ABCA1*) and the basic helix-loop-helix transcription factors, differentiated embryo chondrocyte1 (*DEC1*) and *DEC2*. The rhythms of the mRNA expression levels of *DEC1, DEC2, SREBP-1 and ABCA1* were completely absent in the livers in the ADR group (P<0.05). Although *LXR* and *CYP7A1* maintained circadian rhythm characteristics, the time periods in the ADR group compared with the control rats changed for *LXR* (from 24 h to 12+24 h) and *CYP7A1* (from 4.8 to 24 h; all P<0.05; Fig. 3B).

Functional annotation and PPI network construction. Highly associated genes in a given genetic module serve important roles in biological processes (31). Therefore, the six aforementioned hepatic core clock genes and six clock-controlled genes that were highly associated with the hepatic circadian rhythms of blood lipid metabolism were selected, and PPI networks were constructed using STRING (32). These genes in the PPI network were identified to have stronger interactions among themselves (average local clustering coefficient, 0.849; Fig. 4 and Table III). Notably, the PPI network of STRING v10 makes use of all microarray gene expression experiments deposited in the NCBI Gene Expression Omnibus to provide co-expression analysis, which is a reliable indicator of functional associations (33).

To gain insight into the functional characteristics of the identified blood lipid metabolism-associated protein-coding core clock and clock-controlled genes, GO and KEGG pathway enrichment analyses were performed using DAVID (34). Molecular information was added to GO terms

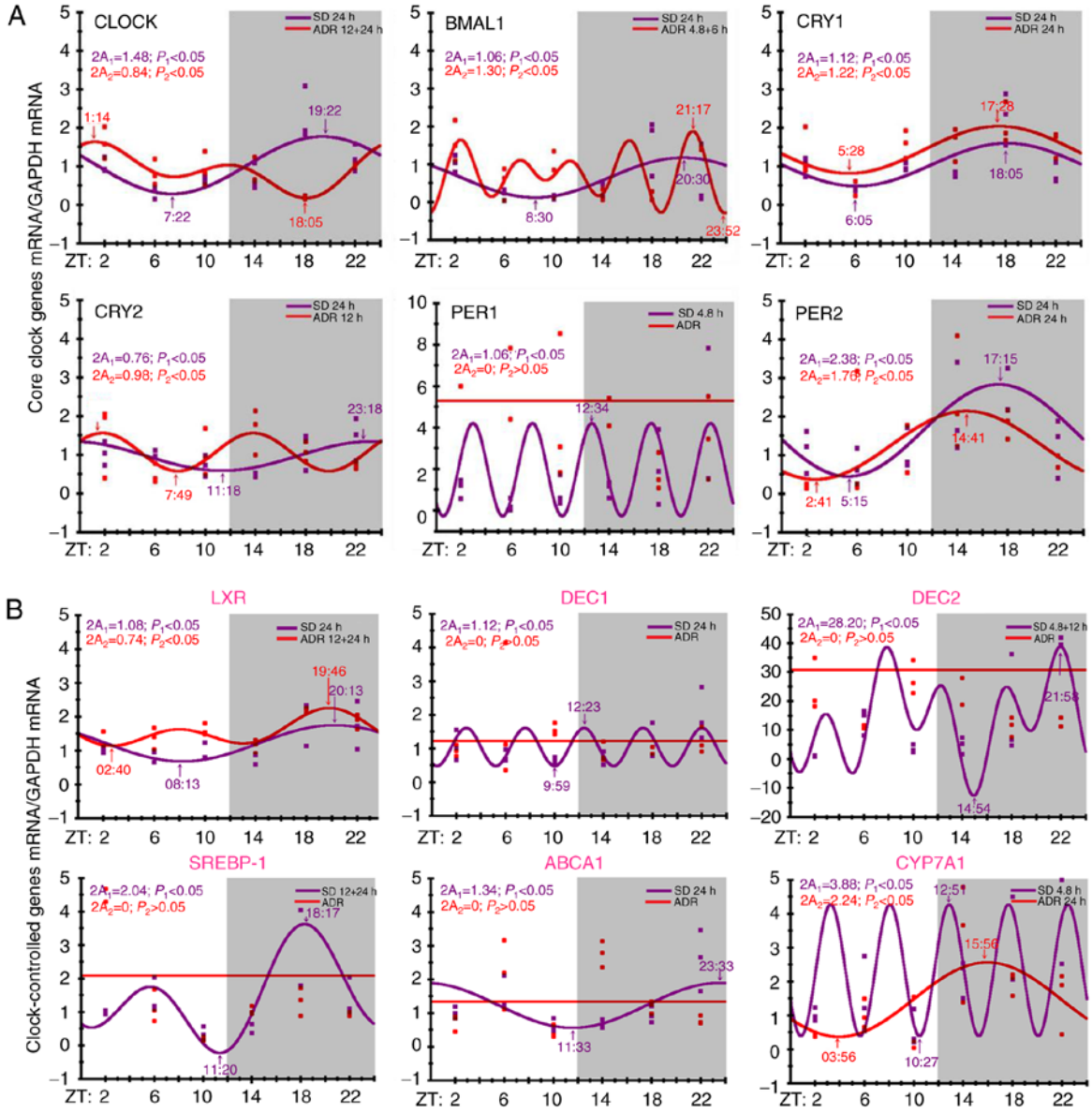

Figure 3. Circadian pattern expressions. (A) Circadian pattern expression of hepatic core clock genes: *CLOCK* and *BMAL*; and two repressors *CRY* and *PER*. (B) Circadian pattern expression of clock-controlled genes: *LXR, CYP7A1, SREBP-1* and *ABCA1*; and the basic helix-loop-helix transcription factors, *DEC1* and *DEC2*. The purple and red dots indicate the measured gene expression values in the control and ADR groups, respectively. ADR, Adriamycin-induced nephropathy; *CLOCK*, circadian locomoter output cycles kaput; *BMAL1*, brain and muscle ARNT-like protein 1; *CRY*, cryptochrome; *PER*, period homologue; *LXR*, liver X receptor; *CYP7A1*, cholesterol 7α-hydroxylase; *SREBP-1*, sterol regulatory element binding protein-1c; *ABCA1*, ATP binding cassette transporter A1; *DEC*, differentiated embryo chondrocyte.

of potential associated genes of circadian rhythms of blood lipid metabolism (Fig. 5). In terms of biological processes, the GO analysis indicated that the clock system protein-coding genes were significantly (all P<0.05) enriched in the circadian regulation of gene expression (GO:0006351), the negative regulation of the glucocorticoid receptor signaling pathway (GO:2000323) and DNA-templated transcription (GO:0045892). In terms of molecular function (MF), the genes were enriched in E-box binding (GO:0070888), transcription factor activity and transcription factor binding (GO:0000989), and transcription regulatory region sequence-specific DNA binding (GO:0000976). Additionally, GO cellular component (CC) analysis revealed that the genes were significantly enriched in the nucleus, chromatoid body and intracellular membrane-bound organelles.

Additionally, a graphic representation of the complicated association between clock genes and the respective GO terms, including a 'concept-and-gene network', was constructed using the GeneAnswers R package (35). To add quantitative molecular data to the GO terms of interest, the GOCircle plot, GOChord and GOCluster plot functions of the *GOplot* R package were added (27) (Figs. 6 and 7). These functions permit the incorporation of data derived from expression level measurements with those obtained from functional annotation enrichment analysis (Table IV).

According to the interactions between the clock genes and the intersecting pathway genes, a clock gene network was constructed that illustrated the network pathway and the key regulatory functions of the identified clock genes. Using KEGG pathway enrichment analysis of Cytoscape and the

Table III. Data of String interactions.

#node1	node2	node1_ string_ internal_id	node2_ string_ internal_id	node1_ external_id	node2_ external_id	neighborhood _on_chromosome	gene_ fusion	phylogenetic_ cooccurrence	Homology	Coexpression	experimentally_ determined_ interaction	database_ annotated	automated_ textmining	combined_ score
CRY2	ARNTL	1860621	1857849	9606.ENSP00000406751	9606.ENSP00000374357	0	0	0	0	0.093	0.98	0.9	0.959	0.999
ARNTL	CRY1	1857849	1842155	9606.ENSP00000374357	9606.ENSP00000008527	0	0	0	0	0.093	0.986	0.9	0.955	0.999
CRY2	PER2	1860621	1844310	9606.ENSP00000406751	9606.ENSP00000254657	0	0	0	0	0.154	0.995	0.9	0.829	0.999
CRY2	PER1	1860621	1849704	9606.ENSP00000406751	9606.ENSP00000314420	0	0	0	0	0.054	0.98	0.9	0.824	0.999
PER1	CRY1	1849704	1842155	9606.ENSP00000314420	9606.ENSP00000008527	0	0	0	0	0.053	0.985	0.9	0.781	0.999
PER2	CRY1	1844310	1842155	9606.ENSP00000254657	9606.ENSP00000008527	0	0	0	0	0.161	0.995	0.9	0.926	0.999
ARNTL	PER1	1857849	1849704	9606.ENSP00000374357	9606.ENSP00000314420	0	0	0	0.626	0	0.967	0.9	0.789	0.997
ARNTL	PER2	1857849	1844310	9606.ENSP00000374357	9606.ENSP00000254657	0	0	0	0.63	0	0.967	0.9	0.968	0.997
PER1	PER2	1849704	1844310	9606.ENSP00000314420	9606.ENSP00000254657	0	0	0	0.844	0.073	0.97	0.9	0.661	0.997
CRY2	CLOCK	1860621	1849105	9606.ENSP00000406751	9606.ENSP00000308741	0	0	0	0	0.053	0.824	0.9	0.835	0.996
CRY2	CRY1	1860621	1842155	9606.ENSP00000406751	9606.ENSP00000008527	0	0	0.527	0.981	0.072	0.967	0.9	0.953	0.996
CLOCK	CRY1	1849105	1842155	9606.ENSP00000308741	9606.ENSP00000008527	0	0	0	0	0.053	0.697	0.9	0.885	0.996
PER2	BHLHE41	1844310	1843637	9606.ENSP00000254657	9606.ENSP00000242728	0	0	0	0	0.053	0.981	0	0.759	0.995
BHLHE41	CRY1	1843637	1842155	9606.ENSP00000242728	9606.ENSP00000008527	0	0	0	0	0.052	0.973	0	0.782	0.993
ARNTL	CLOCK	1857849	1849105	9606.ENSP00000374357	9606.ENSP00000308741	0	0	0	0.687	0.094	0.873	0.9	0.985	0.991
CLOCK	PER2	1849105	1844310	9606.ENSP00000308741	9606.ENSP00000254657	0	0	0	0.61	0.054	0.862	0.9	0.833	0.99
CRY2	BHLHE41	1860621	1843637	9606.ENSP00000406751	9606.ENSP00000242728	0	0	0	0	0.052	0.968	0	0.595	0.987
ARNTL	BHLHE40	1857849	1844442	9606.ENSP00000374357	9606.ENSP00000256495	0	0	0	0	0	0.436	0.9	0.734	0.983
ARNTL	BHLHE41	1857849	1843637	9606.ENSP00000374357	9606.ENSP00000242728	0	0	0	0	0	0.156	0.9	0.764	0.978
NR1H3	ABCA1	1859317	1856172	9606.ENSP00000387946	9606.ENSP00000363868	0	0	0	0	0	0.101	0.9	0.777	0.978
CLOCK	BHLHE41	1849105	1843637	9606.ENSP00000308741	9606.ENSP00000242728	0	0	0	0	0	0.42	0.9	0.621	0.976
PER1	CLOCK	1849704	1849105	9606.ENSP00000314420	9606.ENSP00000308741	0	0	0	0.611	0.051	0.674	0.9	0.591	0.973
CLOCK	BHLHE40	1849105	1844442	9606.ENSP00000308741	9606.ENSP00000256495	0	0	0	0	0	0.178	0.9	0.527	0.957
BHLHE40	BHLHE41	1844442	1843637	9606.ENSP00000256495	9606.ENSP00000242728	0	0	0	0.858	0.181	0.36	0.8	0.759	0.898
NR1H3	SREBF1	1859317	1853255	9606.ENSP00000387946	9606.ENSP00000348069	0	0	0	0	0.049	0.36	0	0.837	0.892
ABCA1	SREBF1	1856172	1853255	9606.ENSP00000363868	9606.ENSP00000348069	0	0	0	0	0	0.088	0	0.838	0.846
BHLHE40	CRY1	1844442	1842155	9606.ENSP00000256495	9606.ENSP00000008527	0	0	0	0	0.052	0.173	0	0.758	0.793
BHLHE40	PER2	1844442	1844310	9606.ENSP00000256495	9606.ENSP00000254657	0	0	0	0	0.053	0.163	0	0.733	0.769
NR1H3	CYP7A1	1859317	1848316	9606.ENSP00000387946	9606.ENSP00000301645	0	0	0	0	0.049	0.079	0	0.742	0.755
ABCA1	CYP7A1	1856172	1848316	9606.ENSP00000363868	9606.ENSP00000301645	0	0	0	0	0	0.046	0	0.694	0.695
SREBF1	CYP7A1	1853255	1848316	9606.ENSP00000348069	9606.ENSP00000301645	0	0	0	0	0.052	0	0	0.673	0.677
NR1H3	ARNTL	1859317	1857849	9606.ENSP00000387946	9606.ENSP00000374357	0	0	0	0	0	0.545	0	0.193	0.617
CRY2	BHLHE40	1860621	1844442	9606.ENSP00000406751	9606.ENSP00000256495	0	0	0	0	0.052	0.173	0	0.52	0.59
SREBF1	BHLHE40	1853255	1844442	9606.ENSP00000348069	9606.ENSP00000256495	0	0	0	0	0	0	0	0.483	0.483
PER1	BHLHE41	1849704	1843637	9606.ENSP00000314420	9606.ENSP00000242728	0	0	0	0	0	0	0	0.422	0.422
PER1	BHLHE40	1849704	1844442	9606.ENSP00000314420	9606.ENSP00000256495	0	0	0	0	0.053	0	0	0.364	0.372
ARNTL	SREBF1	1857849	1853255	9606.ENSP00000374357	9606.ENSP00000348069	0	0	0	0	0	0	0	0.34	0.34
SREBF1	CLOCK	1853255	1849105	9606.ENSP00000348069	9606.ENSP00000308741	0	0	0	0	0	0	0	0.304	0.304
ARNTL	CYP7A1	1857849	1848316	9606.ENSP00000374357	9606.ENSP00000301645	0	0	0	0	0	0	0	0.303	0.303
CLOCK	CYP7A1	1849105	1848316	9606.ENSP00000308741	9606.ENSP00000301645	0	0	0	0	0	0	0	0.25	0.25

Table III. Continued.

#node1	node2	node1_ string_ internal_id	node2_ string_ internal_id	node1_ external_id	node2_ external_id	neighborhood _on_chromosome	gene_ fusion	phylogenetic_ cooccurrence	Homology	Coexpression	experimentally_ determined_ interaction	database_ annotated	automated_ textmining	combined_ score
CYP7A1	CRY1	1848316	1842155	9606.ENSP00000301645	9606.ENSP00000008527	0.074	0	0	0	0	0	0	0.213	0.24
SREBF1	CRY1	1853255	1842155	9606.ENSP00000348069	9606.ENSP00000008527	0	0	0	0	0	0	0	0.233	0.232
CRY2	CYP7A1	1860621	1848316	9606.ENSP00000406751	9606.ENSP00000301645	0.074	0	0	0	0	0	0	0.202	0.229
NR1H3	CLOCK	1859317	1849105	9606.ENSP00000387946	9606.ENSP00000308741	0	0	0	0	0	0	0	0.214	0.214
SREBF1	PER2	1853255	1844310	9606.ENSP00000348069	9606.ENSP00000254657	0	0	0	0	0	0	0	0.211	0.211
CRY2	SREBF1	1860621	1853255	9606.ENSP00000406751	9606.ENSP00000348069	0	0	0	0	0	0	0	0.204	0.204
SREBF1	BHLHE41	1853255	1843637	9606.ENSP00000348069	9606.ENSP00000242728	0	0	0	0	0	0	0	0.203	0.203
NR1H3	BHLHE40	1859317	1844442	9606.ENSP00000387946	9606.ENSP00000256495	0	0	0	0	0	0	0	0.194	0.194
NR1H3	PER2	1859317	1844310	9606.ENSP00000387946	9606.ENSP00000254657	0	0	0	0	0	0	0	0.194	0.194
ABCA1	BHLHE40	1856172	1844442	9606.ENSP00000363868	9606.ENSP00000256495	0	0	0	0	0	0.042	0	0.191	0.191
CYP7A1	BHLHE41	1848316	1843637	9606.ENSP00000301645	9606.ENSP00000242728	0	0	0	0	0	0	0	0.166	0.165
ARNTL	ABCA1	1857849	1856172	9606.ENSP00000374357	9606.ENSP00000363868	0	0	0	0	0.09	0	0	0.111	0.157
CYP7A1	PER2	1848316	1844310	9606.ENSP00000301645	9606.ENSP00000254657	0	0	0	0	0	0	0	0.152	0.151

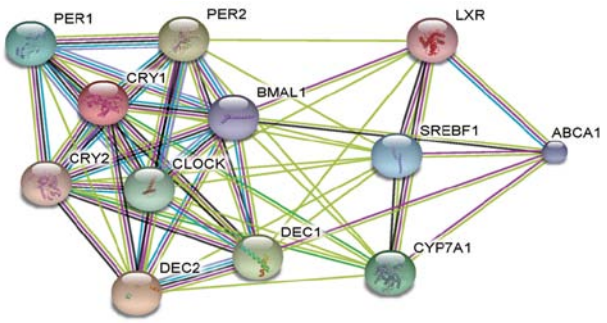

Figure 4. Protein-protein interaction network constructed with the 12 clock and clock-controlled genes. Genes were enriched in the differential pathways identified in the *Homo sapiens* genome (avg. local clustering coefficient, 0.849). The colored nodes/lines represent different proteins/protein-protein interactions.

KOBAS network, the rhythmically expressed protein-coding genes were determined to be significantly enriched in circadian rhythm (hsa04710), PPAR signaling pathways (hsa03320), circadian entrainment (hsa04713), fat digestion and absorption (hsa04975) and ABC transporters (hsa02010); Fig. 8 and Table V).

Discussion

The majority of studies suggest that the lipid metabolism involved in kidney disease primarily affects local tissue lipid deposition and local tissue energy barriers (36). However, serum cholesterol levels of patients with CKD are determined by endogenous synthesis and intestinal absorption of exogenous cholesterol (37). Although numerous tissues (endocrine organs, the immune system, the endothelium) contribute to the plasma protein pool, the bulk of plasma proteins is secreted by the liver and are those lost to the highest extent in the NS (38). Additionally, three-quarters of the total cholesterol is synthesized in the liver (39), thus, it was hypothesized that renal injury affects peripheral blood lipid levels through the liver. Therefore, the present study focused on the hepatic clock system that affects circulating lipids.

Clinicians usually overlook the circadian rhythm of blood lipids. Few primary research studies have explored the circadian rhythm of blood lipids (40-42). However, previous studies have suggested that the deletion or knockdown of mouse core clock genes results in several circadian rhythm abnormalities concerning TGs, gluconeogenesis and liver GLU metabolism (40,43). It is well acknowledged that hyperlipidemia occurs in patients with NS and improves immediately with the remission of NS. It is an excellent model of kidney disease to explore the circadian rhythm of blood lipids, and the underlying crosstalk between kidney and liver.

In the present study, nephropathy induced by ADR in rats presented with the typical characteristics of normal renal function, hypoalbuminemia and hyperlipidemia. Electron microscopy indicated partial podocyte fusion, which is a major cause of idiopathic NS. Multiple and large doses (total >10 mg/kg) of Adriamycin are associated with the development of rat hepatic lesions (44), whereby Adriamycin causes significant abnormalities in liver function parameters. In previous studies, the single dose of Adriamycin generally used

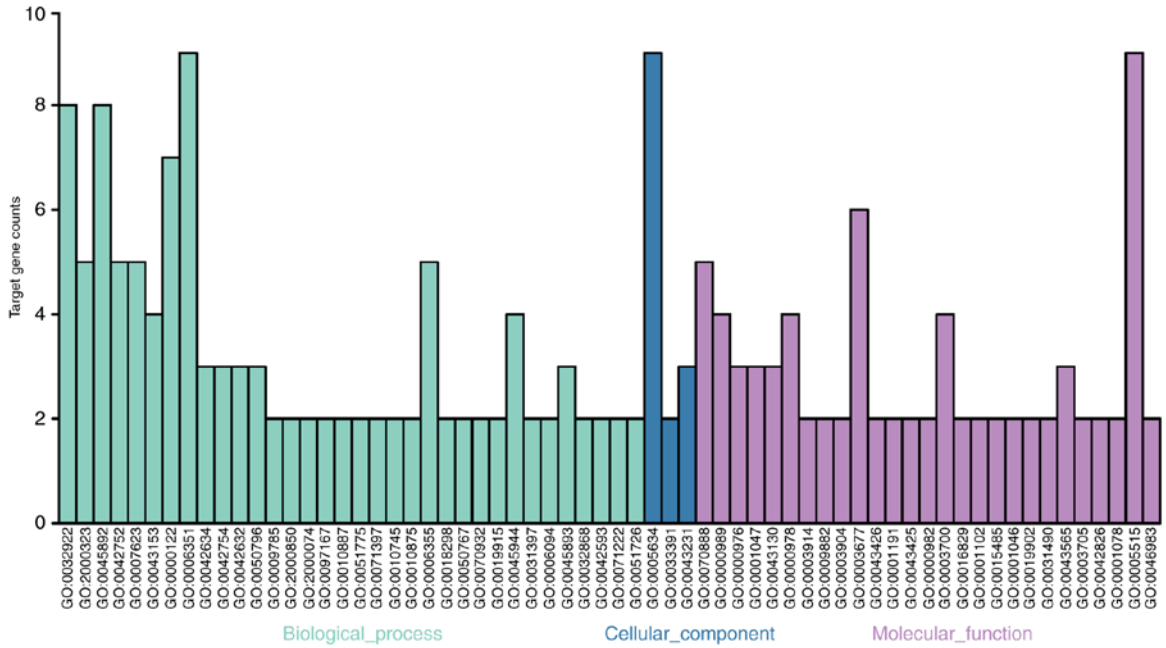

Figure 5. Target gene counts of GO biological processes. The GO analysis results demonstrated that the clock system protein-coding genes were significantly enriched in the circadian regulation of gene expression (GO:0006351), negative regulation of glucocorticoid receptor signaling pathway (GO:2000323) and DNA-templated (GO:0045892) under BPs (light blue bar). Under MF (purple), the genes were enriched in E-box binding (GO:0070888), transcription factor activity, transcription factor binding (GO:0000989) and transcription regulatory region sequence-specific DNA binding (GO:0000976). Additionally, GO CC (dark blue bar) analysis revealed genes significantly were enriched in the nucleus, chromatoid body and the intracellular membrane-bounded organelle. GO, Gene Ontology; BP, biological process; CC, cellular component; MF, molecular function.

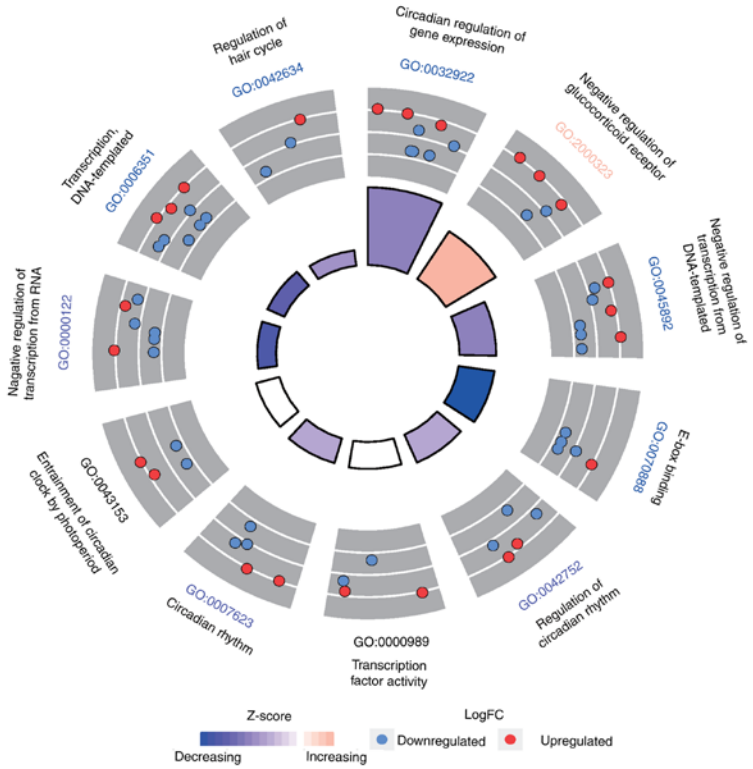

Figure 6. Functional characterization of differentially and rhythmically expressed protein-coding genes. GOCircle plot: The outer circle shows a scatter plot of the expression levels of rhythmically expressed clock-associated genes in each enriched GO term. Red circles indicate upregulation and blue circles indicate downregulation. The inner ring is a bar plot, where the height of the bar indicates the significance of the GO term (log10-adjusted P-value), and the color corresponds to the z-score: blue, decreased; red, increased; and white, unchanged. GO, Gene Ontology.

in rats to induce NS is between 5.0 and 7.5 mg/kg (16,45,46). Since complete absorption of the drug may induce organ damage, intravenous injection provides direct access to the drug and eliminates the absorption dependence on the

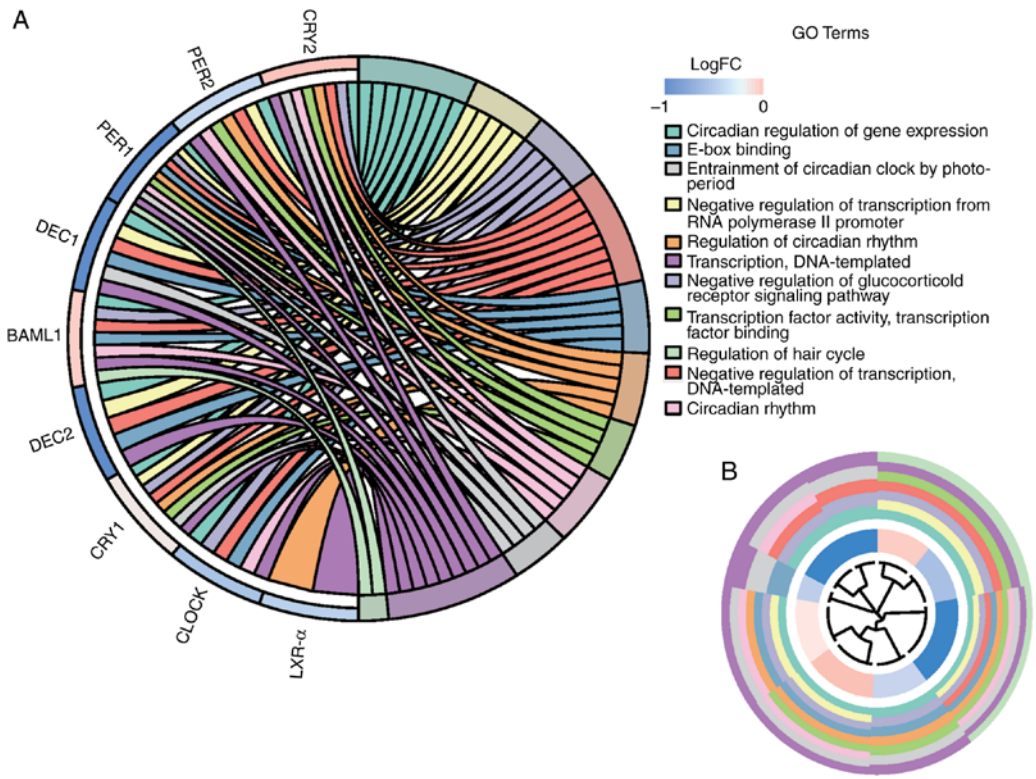

Figure 7. Specific clock genes are involved in pathways. (A) GOChord plot: A plot indicated the association between statistically significant clock genes and their associated GO terms; the genes are associated via ribbons to their assigned terms. Blue-to-red coding next to the selected genes indicates the amplitude change (the difference between the expression amplitude in the two groups divided by the amplitude of the control group). A negative sign indicates a decrease and a positive sign indicates an increase. The outer ring shows the assigned functional terms. (B) GOCluster plot: A circular dendrogram of the clustering of the expression profiles. The inner ring shows the color-coded amplitude changes and the outer ring shows the assigned functional terms. The details are provided in Table IV.

peritoneal membrane (46). Therefore, the present study used a single tail vein injection dose of 6.5 mg/kg the day after 2 weeks of adaptation and particular caution was taken due to the risk of extravasation during injection. The ADR-induced nephropathy rats exhibited significantly higher blood lipid levels and a disturbed blood lipid circadian rhythm ($P<0.05$). Notably, the activities of AST and ALT in the ADR group were not pathologically increased, whereby the levels were within the normal range of male rats aged 12-13 weeks (normal ranges: AST, 87-144 U/l; ALT, 28-40 U/l) (23). The NS rats in the present study may not have experienced deterioration in hepatic function, because the levels of ALT and AST remained within the normal range compared with the control group, and the total dose of Adriamycin was less than the dose required to induce liver damage. Dyslipidemia may be attributed to the compensatory liver dysfunction under the nephritic state. However, the lack of histological staining of liver tissue in the same set of experiments was a limitation of this study.

Multiple regulators of lipid metabolism and rate-limiting enzymes in TG accumulation exhibit circadian rhythmicity during nutrient metabolism, and the clock system is indispensable for these processes in the liver. Mice lacking the liver-specific core clock gene *BMAL1* exhibit abnormalities in blood TGs, GLU and gluconeogenesis. Furthermore, a previous study revealed the metabolism-associated clock-controlled genes altered rhythms; however, the rhythm of GLU remained consistent in the asynchronous dietary (47). Human plasma lipid levels, including those of TGs and cholesterol, are rhythmic over a 24-h period (48), independent of feeding and waking conditions (42). Furthermore, Chua *et al* (42) did not detect a circadian rhythm in blood GLU and LDL-C; however, a trend was observed for higher levels of LDL-C during the daytime, this may be due to substantial individual differences in timing of the rhythm. Their results are consistent with the present study; however, they did not evaluate a rhythmic component via the Fourier transform method. Significant daily variations in the HDL-C levels were detected by Rivera-Coll *et al* (48) and Van den Berg *et al* (49). However, Van Den Berg *et al* (49) did not evaluate a rhythmic component. Notably, different analytical methods in other studies make it difficult to compare the result that lack of circadian rhythm associated with HDL-C levels in the present study; a fact that may explain, in part, the observed differences in timing and daily amplitude between the present research and other studies. A previous study indicated *CLOCK* knockout mice exhibit hyperlipidemia and hepatic steatosis, and *PER1* regulates *PPARα* mRNA expression and the development of obesity (41). Furthermore, *PER2* has been suggested to be involved in PPAR-associated pathways and white adipose tissue mobilization (3). The aforementioned studies suggested that different circadian clock genes serve a role in the regulation of lipid regulation.

In the present study, the mRNA expression of six hepatic core clock genes in the normal control group was associated with stable rhythmic features, with minimums during the day and maximums at night (activity period), which is consistent with previous studies on mice (50,51). Furthermore, the cycle

Table IV. Data of GO biological processes.

Category	Term	Count	%	P-value	Genes	List total	Pop hits	Pop total	Fold enrichment	Bonferroni	Benjamini	FDR
GOTERM_BP_DIRECT	GO:0032922~circadian regulation of gene expression	8	72.73	$4.21x10^{-16}$	CRY2, PER2, PER1, BHLHE40, ARNTL, BHLHE41, CRY1, CLOCK	11	57	16792	214.25	$6.48x10^{-14}$	$6.48x10^{-14}$	$5.33x10^{-13}$
GOTERM_BP_DIRECT	GO:2000323~negative regulation of glucocorticoid receptor signaling pathway	5	45.45	$9.51x10^{-13}$	CRY2, PER1, ARNTL, CRY1, CLOCK	11	6	16792	1,272.12	$1.39x10^{-10}$	$6.94x10^{-11}$	$1.13x10^{-09}$
GOTERM_BP_DIRECT	GO:0045892~negative regulation of transcription, DNA-templated	8	72.73	$2.18x10^{-09}$	CRY2, PER2, PER1, BHLHE40, ARNTL, BHLHE41, CRY1, CLOCK	11	499	16792	24.47	$3.18x10^{-07}$	$1.06x10^{-07}$	$2.59x10^{-06}$
GOTERM_MF_DIRECT	GO:0070888~E-box binding	5	45.45	$2.85x10^{-09}$	PER1, BHLHE40, ARNTL, BHLHE41, CLOCK	11	34	16881	225.68	$2.08x10^{-07}$	$2.08x10^{-07}$	$2.98x10^{-06}$
GOTERM_BP_DIRECT	GO:0042752~regulation of circadian rhythm	5	45.45	$1.33x10^{-08}$	CRY2, PER2, PER1, CRY1, NR1H3	11	49	16792	155.77	$1.94x10^{-06}$	$4.84x10^{-07}$	$1.58x10^{-05}$
GOTERM_MF_DIRECT	GO:0000989~transcription factor activity, transcription factor binding	4	36.36	$5.43x10^{-08}$	CRY2, PER2, PER1, CRY1	11	14	16881	438.47	$3.96x10^{-06}$	$1.98x10^{-06}$	$5.67x10^{-05}$
GOTERM_BP_DIRECT	GO:0007623~circadian rhythm	5	45.45	$7.55x10^{-08}$	CRY2, PER2, PER1, ARNTL, CLOCK	11	75	16792	101.77	$1.10x10^{-05}$	$2.21x10^{-06}$	$8.98x10^{-05}$
GOTERM_BP_DIRECT	GO:0043153~entrainment of circadian clock by photoperiod	4	36.36	$1.72x10^{-07}$	CRY2, PER1, BHLHE40, CRY1	11	20	16792	305.31	$2.52x10^{-05}$	$4.20x10^{-06}$	$2.05x10^{-04}$
GOTERM_BP_DIRECT	GO:0000122~negative regulation of transcription from RNA polymerase II promoter	7	63.64	$1.10x10^{-06}$	CRY2, PER2, PER1, BHLHE40, BHLHE41, CRY1, NR1H3	11	720	16792	14.84	$1.61x10^{-04}$	$2.30x10^{-05}$	$1.31x10^{-03}$
GOTERM_BP_DIRECT	GO:0006351~transcription, DNA-templated	9	81.82	$1.21x10^{-06}$	CRY2, PER2, PER1, BHLHE40, ARNTL, BHLHE41, CRY1, CLOCK, NR1H3	11	1955	16792	7.03	$1.76x10^{-04}$	$2.20x10^{-05}$	$1.43x10^{-03}$
GOTERM_BP_DIRECT	GO:0042634~regulation of hair cycle	3	27.27	$3.19x10^{-06}$	PER1, ARNTL, CLOCK	11	5	16792	915.92	$4.65x10^{-04}$	$5.17x10^{-05}$	$3.79x10^{-03}$
GOTERM_BP_DIRECT	GO:0042754~negative regulation of circadian rhythm	3	27.27	$1.15x10^{-05}$	CRY2, PER2, CRY1	11	9	16792	508.85	$1.67x10^{-03}$	$1.67x10^{-04}$	$1.36x10^{-02}$
GOTERM_MF_DIRECT	GO:0000976~transcription regulatory region sequence-specific DNA binding	3	27.27	$5.13x10^{-04}$	CRY2, PER2, ARNTL	11	58	16881	79.38	$3.68x10^{-02}$	$1.24x10^{-02}$	$5.34x10^{-01}$
GOTERM_MF_DIRECT	GO:0001047~core promoter binding	3	27.27	$6.24x10^{-04}$	ARNTL, CRY1, CLOCK	11	64	16881	71.94	$4.46x10^{-02}$	$1.13x10^{-02}$	$6.50x10^{-01}$
GOTERM_BP_DIRECT	GO:0042632~cholesterol homeostasis	3	27.27	$6.31x10^{-04}$	CYP7A1, ABCA1, NR1H3	11	64	16792	71.56	$8.80x10^{-02}$	$8.34x10^{-03}$	$7.47x10^{-01}$
GOTERM_BP_DIRECT	GO:0050796~regulation of insulin secretion	3	27.27	$6.91x10^{-04}$	PER2, ARNTL, CLOCK	11	67	16792	68.35	$9.60x10^{-02}$	$8.38x10^{-03}$	$8.19x10^{-01}$
GOTERM_MF_DIRECT	GO:0043130~ubiquitin binding	3	27.27	$9.26x10^{-04}$	CRY2, PER2, CRY1	11	78	16881	59.02	$6.54x10^{-02}$	$1.34x10^{-02}$	$9.62x10^{-01}$
GOTERM_MF_DIRECT	GO:0000978~RNA polymerase II core promoter proximal region sequence-specific DNA binding	4	36.36	$9.91x10^{-04}$	PER1, BHLHE41, CLOCK, NR1H3	11	355	16881	17.29	$6.99x10^{-02}$	$1.20x10^{-02}$	1.03

Table IV. Continued.

Category	Term	Count	%	P-value	Genes	List total	Pop hits	Pop total	Fold enrichment	Bonferroni	Benjamini	FDR
GOTERM_MF_DIRECT	GO:0003904~deoxyribodipyrimidine photo-lyase activity	2	18.18	$1.18x10^{-03}$	CRY2, CRY1	11	2	16881	1,534.64	$8.29 x10^{-02}$	$1.23x10^{-02}$	1.23
GOTERM_MF_DIRECT	GO:0003914~DNA (6-4) photolyase activity	2	18.18	$1.18x10^{-03}$	CRY2, CRY1	11	2	16881	1,534.64	$8.29x10^{-02}$	$1.23x10^{-02}$	1.23
GOTERM_MF_DIRECT	GO:0009882~blue light photoreceptor activity	2	18.18	$1.18x10^{-03}$	CRY2, CRY1	11	2	16881	1,534.64	$8.29x10^{-02}$	$1.23x10^{-02}$	1.23
GOTERM_BP_DIRECT	GO:0009785~blue light signaling pathway	2	18.18	$1.19x10^{-03}$	CRY2, CRY1	11	2	16792	1,526.55	$1.60x10^{-01}$	$1.33x10^{-02}$	1.41
GOTERM_BP_DIRECT	GO:2000850~negative regulation of glucocorticoid secretion	2	18.18	$1.19x10^{-03}$	CRY2, CRY1	11	2	16792	1,526.55	$1.60x10^{-01}$	$1.33x10^{-02}$	1.41
GOTERM_CC_DIRECT	GO:0005634~nucleus	9	81.81	$1.48x10^{-03}$	CRY2, PER2, PER1, BHLHE40, ARNTL, BHLHE41, CRY1, CLOCK, NR1H3	11	5415	18224	2.75	$3.63x10^{-02}$	$3.63x10^{-02}$	1.19
GOTERM_MF_DIRECT	GO:0003677~DNA binding	6	54.55	$1.57x10^{-03}$	CRY2, ARNTL, BHLHE41, CRY1, CLOCK, NR1H3	11	1674	16881	5.50	$1.08x10^{-01}$	$1.42x10^{-02}$	1.62
GOTERM_BP_DIRECT	GO:2000074~regulation of type B pancreatic cell development	2	18.18	$1.79x10^{-03}$	ARNTL, CLOCK	11	3	16792	1,017.70	$2.30x10^{-01}$	$1.85x10^{-02}$	2.10
GOTERM_BP_DIRECT	GO:0097167~circadian regulation of translation	2	18.18	$2.39x10^{-03}$	PER2, PER1	11	4	16792	763.27	$2.94x10^{-01}$	$2.29x10^{-02}$	2.79
GOTERM_MF_DIRECT	GO:0043426~MRF binding	2	18.18	$2.96x10^{-03}$	BHLHE40, BHLHE41	11	5	16881	613.85	$1.95x10^{-01}$	$2.37x10^{-02}$	3.05
GOTERM_BP_DIRECT	GO:0010887~negative regulation of cholesterol storage	2	18.18	$3.57x10^{-03}$	ABCA1, NR1H3	11	6	16792	508.85	$4.07x10^{-01}$	$3.21x10^{-02}$	4.16
GOTERM_BP_DIRECT	GO:0051775~response to redox state	2	18.18	$5.94x10^{-03}$	ARNTL, CLOCK	11	10	16792	305.31	$5.81x10^{-01}$	$4.99x10^{-02}$	6.84
GOTERM_CC_DIRECT	GO:0033391~chromatoid body	2	18.18	$6.57x10^{-03}$	ARNTL, CLOCK	11	12	18224	276.12	$1.52x10^{-01}$	$7.91x10^{-02}$	5.21
GOTERM_MF_DIRECT	GO:0001191~transcriptional repressor activity, RNA polymerase II transcription factor binding	2	18.18	$7.09x10^{-03}$	BHLHE40, BHLHE41	11	12	16881	255.77	$4.05x10^{-01}$	$5.06x10^{-02}$	7.16
GOTERM_BP_DIRECT	GO:0071397~cellular response to cholesterol	2	18.18	$7.13x10^{-03}$	CYP7A1, ABCA1	11	12	16792	254.42	$6.48x10^{-01}$	$5.64x10^{-02}$	8.15
GOTERM_BP_DIRECT	GO:0010745~negative regulation of macrophage derived foam cell differentiation	2	18.18	$7.72x10^{-03}$	ABCA1, NR1H3	11	13	16792	234.85	$6.77x10^{-01}$	$5.78x10^{-02}$	8.80
GOTERM_BP_DIRECT	GO:0010875~positive regulation of cholesterol efflux	2	18.18	$8.31x10^{-03}$	ABCA1, NR1H3	11	14	16792	218.08	$7.04x10^{-01}$	$5.91x10^{-02}$	9.44
GOTERM_BP_DIRECT	GO:0006355~regulation of transcription, DNA-templated	5	45.45	$8.66x10^{-03}$	BHLHE40, ARNTL, BHLHE41, CLOCK, NR1H3	11	1504	16792	5.07	$7.19x10^{-01}$	$5.87x10^{-02}$	9.82
GOTERM_BP_DIRECT	GO:0018298~protein-chromophore linkage	2	18.18	$9.50x10^{-03}$	CRY2, CRY1	11	16	16792	190.82	$7.51x10^{-01}$	$6.13x10^{-02}$	10.71

Table IV. Continued.

Category	Term	Count	%	P-value	Genes	List total	Pop hits	Pop total	Fold enrichment	Bonferroni	Benjamini	FDR
GOTERM_BP_DIRECT	GO:0050767~regulation of neurogenesis	2	18.18	$1.13x10^{-02}$	PER2, ARNTL	11	19	16792	160.69	$8.09x10^{-01}$	$6.94x10^{-02}$	12.59
GOTERM_BP_DIRECT	GO:0070932~histone H3 deacetylation	2	18.18	$1.24x10^{-02}$	PER2, PER1	11	21	16792	145.39	$8.39x10^{-01}$	$7.33x10^{-02}$	13.82
GOTERM_MF_DIRECT	GO:0000982~transcription factor activity, RNA polymerase II core promoter proximal region sequence-specific binding	2	18.18	$1.35x10^{-02}$	ARNTL, CLOCK	11	23	16881	133.45	$6.30x10^{-01}$	$8.65x10^{-02}$	13.27
GOTERM_MF_DIRECT	GO:0043425~bHLH transcription factor binding	2	18.18	$1.35x10^{-02}$	BHLHE40, BHLHE41	11	23	16881	133.45	$6.30x10^{-01}$	$8.65x10^{-02}$	13.27
GOTERM_BP_DIRECT	GO:0019915~lipid storage	2	18.18	$1.42x10^{-02}$	CRY2, CRY1	11	24	16792	127.21	$8.76x10^{-01}$	$8.02x10^{-02}$	15.63
GOTERM_MF_DIRECT	GO:0003700~transcription factor activity, sequence-specific DNA binding	4	36.36	$1.63x10^{-02}$	BHLHE40, ARNTL, CLOCK, NR1H3	11	961	16881	6.39	$6.99x10^{-01}$	$9.53x10^{-02}$	15.78
GOTERM_BP_DIRECT	GO:0045944~positive regulation of transcription from RNA polymerase II promoter	4	36.36	$1.75x10^{-02}$	PER1, ARNTL, CLOCK, NR1H3	11	981	16792	6.22	$9.24x10^{-01}$	$9.44x10^{-02}$	18.93
GOTERM_MF_DIRECT	GO:0016829~lyase activity	2	18.18	$1.88x10^{-02}$	CRY2, CRY1	11	32	16881	95.91	$7.50x10^{-01}$	$1.01x10^{-01}$	17.97
GOTERM_MF_DIRECT	GO:0001102~RNA polymerase II activating transcription factor binding	2	18.18	$2.23x10^{-02}$	BHLHE40, BHLHE41	11	38	16881	80.77	$8.07x10^{-01}$	$1.11x10^{-01}$	20.97
GOTERM_MF_DIRECT	GO:0015485~cholesterol binding	2	18.18	$2.40x10^{-02}$	ABCA1, NR1H3	11	41	16881	74.86	$8.31x10^{-01}$	$1.12x10^{-01}$	22.42
GOTERM_BP_DIRECT	GO:0031397~negative regulation of protein ubiquitination	2	18.18	$2.42x10^{-02}$	PER2, CRY1	11	41	16792	74.47	$9.72x10^{-01}$	$1.24x10^{-01}$	25.22
GOTERM_MF_DIRECT	GO:0001046~core promoter sequence-specific DNA binding	2	18.18	$2.52x10^{-02}$	CRY1, CLOCK	11	43	16881	71.38	$8.45x10^{-01}$	$1.10x10^{-01}$	23.38
GOTERM_BP_DIRECT	GO:0006094~gluconeogenesis	2	18.18	$2.59x10^{-02}$	PER2, CRY1	11	44	16792	69.39	$9.78x10^{-01}$	$1.28x10^{-01}$	26.80
GOTERM_MF_DIRECT	GO:0019902~phosphatase binding	2	18.18	$2.63x10^{-02}$	CRY2, CRY1	11	45	16881	68.21	$8.58x10^{-01}$	$1.08x10^{-01}$	24.32
GOTERM_MF_DIRECT	GO:0031490~chromatin DNA binding	2	18.18	$3.38x10^{-02}$	PER1, CLOCK	11	58	16881	52.92	$9.19x10^{-01}$	$1.30x10^{-01}$	30.17
GOTERM_CC_DIRECT	GO:0043231~intracellular membrane-bounded organelle	3	27.27	$3.58x10^{-02}$	CYP7A1, ARNTL, CLOCK	11	558	18224	8.91	$5.98x10^{-01}$	$2.62x10^{-01}$	25.59
GOTERM_BP_DIRECT	GO:0045893~positive regulation of transcription, DNA-templated	3	27.27	$3.59x10^{-02}$	ARNTL, CLOCK, NR1H3	11	515	16792	8.89	$9.95x10^{-01}$	$1.68x10^{-01}$	35.24
GOTERM_MF_DIRECT	GO:0043565~sequence-specific DNA binding	3	27.27	$3.59x10^{-02}$	ARNTL, CLOCK, NR1H3	11	518	16881	8.89	$9.31x10^{-01}$	$1.31x10^{-01}$	31.74
GOTERM_MF_DIRECT	GO:0003705~transcription factor activity, RNA polymerase II distal enhancer sequence-specific binding	2	18.18182	$3.84x10^{-02}$	BHLHE40, BHLHE41	11	66	16881	46.50	$9.43x10^{-01}$	$1.33x10^{-01}$	33.57
GOTERM_BP_DIRECT	GO:0032868~response to insulin	2	18.18	$3.92x10^{-02}$	CRY2, CRY1	11	67	16792	45.57	$9.97x10^{-01}$	$1.77x10^{-01}$	37.83
GOTERM_BP_DIRECT	GO:0042593~glucose homeostasis	2	18.18	$5.86x10^{-02}$	CRY2, CRY1	11	101	16792	30.22	$9.99x10^{-01}$	$2.47x10^{-01}$	51.19

Table IV. Continued.

Category	Term	Count	%	P-value	Genes	List total	Pop hits	Pop total	Fold enrichment	Bonferroni	Benjamini	FDR
GOTERM_MF_DIRECT	GO:0042826~histone deacetylase binding	2	18.18	$5.88x10^{-02}$	BHLHE41, CRY1	11	102	16881	30.09	$9.88x10^{-01}$	$1.90x10^{-01}$	46.89
GOTERM_MF_DIRECT	GO:0001078~transcriptional repressor activity, RNA polymerase II core promoter proximal region sequence-specific binding	2	18.18	$6.39x10^{-02}$	BHLHE40, BHLHE41	11	111	16881	27.65	$9.92x10^{-01}$	$1.97x10^{-01}$	49.78
GOTERM_BP_DIRECT	GO:0071222~cellular response to lipopolysaccharide	2	18.18	$6.53x10^{-02}$	ABCA1, NR1H3	11	113	16792	27.02	$9.99x10^{-01}$	$2.65x10^{-01}$	55.19
GOTERM_MF_DIRECT	GO:0005515~protein binding	9	81.82	$7.05x10^{-02}$	CRY2, PER2, BHLHE40, ARNTL, ABCA1, BHLHE41, CRY1, CLOCK, NR1H3	11	8785	16881	1.57	$9.95x10^{-01}$	$2.07x10^{-01}$	53.38
GOTERM_BP_DIRECT	GO:0051726~regulation of cell cycle	2	18.18	$7.15x10^{-02}$	PER2, ARNTL	11	124	16792	24.62	$9.99x10^{-01}$	$2.80x10^{-01}$	58.57
GOTERM_MF_DIRECT	GO:0046983~protein dimerization activity	2	18.18	$8.55x10^{-02}$	ARNTL, CLOCK	11	150	16881	20.46	$9.99x10^{-01}$	$2.38x10^{-01}$	60.62

GO, Gene Ontology; FDR, false discovery rate.

duration was 24 h for five core clock genes (*CLOCK*, *BMAL1*, *PER2*, *CRY1* and *CRY2*) and 12 h for *PER1* in the control group. However, extended or abnormal rhythms were exhibited in the ADR group. Although *PER1* mRNA was expressed in the ADR group, the rhythm was absent ($P<0.05$). In addition, disordered rhythms were revealed in the downstream lipid-associated clock-controlled genes of core hepatic clock genes (*LXR*, *DEC1*, *DEC2*, *SREBP-1*, *ABCA1* and *CYP7A1*). Among these, the rhythmic expression of functional clock genes (*DEC1* and *DEC2*), as well as *PER1,* was entirely absent in the ADR group. Notably, the former two genes are downstream of the core clock gene *PER1* and regulate feedback of *PER1* transcription (52). *CYP7A1*, *SREBP-1* and *ABCA1* all exhibit periodic oscillations, and are regulated by *DEC1* and *DEC2* (53). CYP7α serves important roles in bile acid synthesis and its rhythmic expression is inhibited by binding DEC2 via E-box elements. The present finding supports that increasing hepatic *DEC2* mRNA expression may result in a reduction in *CYP7α* mRNA expression in NS rats. This may hinder the metabolism of cholesterol into bile acids, thereby inducing the occurrence of hypercholesterolemia. LXRα increases *CYP7α* expression and promotes bile acid synthesis (54). ABCA1 typically mediates the transmembrane transport of lipids metabolites (55), serving a key role in the reverse transport of cholesterol *in vivo*. It also permits intracellular cholesterol, phospholipid and free ApoA or ApoE binding to LXRα, which then initiates HDL synthesis. In addition, several fatty acid synthase genes are target genes of *SREBP-1*, and the activity of *SREBP-1* leads to an increase in blood TG synthesis. The present study indicated that the circadian rhythmic expression of lipid metabolism genes was regulated by the critical rhythm of key enzymes and transcription-associated factors, and the associated fat synthase gene was simultaneously activated by the core clock genes (Fig. 9).

Due to the limitation that human liver tissue cannot be extracted six times within 24 h to monitor blood lipid rhythm analysis, GO and KEGG enrichment assays were performed to detect differentially expressed clock genes to provide a biologically meaningful explanation of the present results in humans. Using bioinformatics methods, including the GOplot R package, for visually combining expression data with functional analysis and predicting the potential disease-causing genes has been considered viable in various diseases (56,57). The enrichment of GO annotation terms revealed that the clock system protein-coding genes were significantly enriched in specific biological processes, MFs and CCs. In particular, the most representative functional processes of clock genes were the circadian regulation of gene expression, E-box binding, transcription factor activity and negative regulation of the glucocorticoid receptor signaling pathway. These findings were consistent with previous evidence that suggest the essential role of these pathogenetic mechanisms in disease states (4,5,9). However, the most significant limitation of the current research is the observational nature of the study *in vivo*, and the lack of specific knockdown and response experiments.

The functional interpretation of the GO- and KEGG-based clock-specific 'concept-and-gene networks' in the present study highlighted the possibility that core clock genes exert pathogenic effects via different multifactorial combinations, providing an important insight into clock core

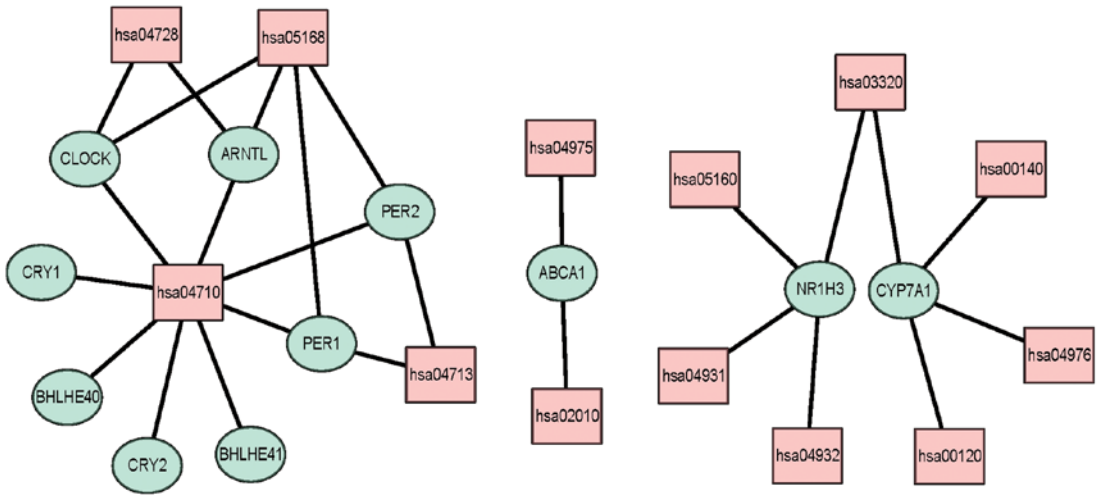

Figure 8. KEGG analysis was conducted using KOBAS 3.0 online software (http://kobas.cbi.pku.edu.cn/). KEGG pathway enrichment of significant rhythmically expressed protein-coding genes. The green node represents significant rhythmically expressed protein-coding genes. The red node represents enriched pathway symbols. The details are provided in Table V. KEGG, Kyoto Encyclopedia of Genes and Genomes.

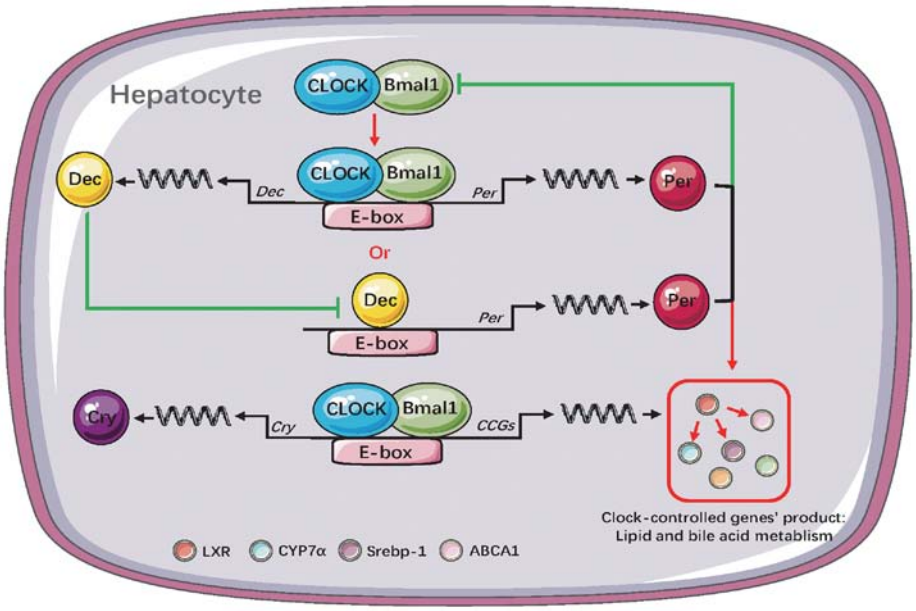

Figure 9. Diagram of liver clock gene and clock control gene association. The red line represents the promoting effect, the green line represents inhibition, and the black line represents transcription into protein. *CLOCK*, circadian locomoter output cycles kaput; *BMAL1*, brain and muscle ARNT-like protein 1; *CRY*, cryptochrome; *PER*, period homologue; *LXR*, liver X receptor; *CYP7A1*, cholesterol 7α-hydroxylase; *SREBP-1*, sterol regulatory element binding protein-1c; *ABCA1*, ATP binding cassette transporter A1; *DEC*, differentiated embryo chondrocyte.

genes that may have a fundamental influence in NS. The transcriptional amplitude of clock genes was decreased or absent in patients with NS included in this study, suggesting that these proteins may represent susceptibility factors for disordered rhythms.

To compensate for the difficulties and limitations of human circadian rhythm research, multiple bioinformatics methods were used to analyze the associations between the overall human core clock (*BMAL1*, *CLOCK*, *CRY1*, *CRY2*, *PER1* and *PER2*) and clock-controlled genes (*LXR*, *DEC1*, *DEC2*, *SREBP-1*, *ABCA1* and *CYP7A1*), including signaling pathway and correlation prediction analyses. Their associations in the co-expression network were determined (avg. local clustering coefficient, 0.849). Consistent with the KEGG pathway analysis results, these genes were primarily enriched in the circadian rhythm pathway, and governed the regulation of downstream liver-specific, lipid-associated clock-controlled genes and blood lipid homeostasis and rhythmicity. These results may aid in providing a deeper understanding of rhythmic gene expression in the human clock system.

From the publications reviewed, NS is one of the few acquired conditions that alter the plasma levels of lipoprotein (58). Once NS enters remission, lipoprotein levels normalize quickly (38), and the changes in hepatic circadian rhythm were demonstrated to be secondary to kidney disease without any damage to liver tissue in the present study. Since the molecular mechanism of the circadian rhythm of an organism involves the clock gene system, and the activity of

Table V. Data of KEGG pathways analysis.

Term	Database	ID	Input number	Background number	P-value	Corrected P-value	Input	Hyperlink
Circadian rhythm	KEGG PATHWAY	hsa04710	8	31	6.53×10^{-23}	9.80×10^{-22}	8864|5187|8553|406|1408|9575|79365|1407	http://www.genome.jp/kegg-bin/show_pathway?hsa04710/hsa:8553%09red/hsa:9575%09red/hsa:406%09red/hsa:1408%09red/hsa:5187%09red/hsa:8864%09red/hsa:79365%09red/hsa:1407%09red
Herpes simplex infection	KEGG PATHWAY	hsa05168	4	186	1.62×10^{-07}	1.22×10^{-06}	406|8864|5187|9575	http://www.genome.jp/kegg-bin/show_pathway?hsa05168/hsa:9575%09red/hsa:406%09red/hsa:8864%09red/hsa:5187%09red
PPAR signaling pathway	KEGG PATHWAY	hsa03320	2	72	1.86×10^{-04}	9.29×10^{-04}	10062|1581	http://www.genome.jp/kegg-bin/show_pathway?hsa03320/hsa:1581%09red/hsa:10062%09red
Circadian entrainment	KEGG PATHWAY	hsa04713	2	95	3.19×10^{-04}	1.20×10^{-04}	8864|5187	http://www.genome.jp/kegg-bin/show_pathway?hsa04713/hsa:8864%09red/hsa:5187%09red
Dopaminergic synapse	KEGG PATHWAY	hsa04728	2	130	5.90×10^{-04}	1.77×10^{-03}	406|9575	http://www.genome.jp/kegg-bin/show_pathway?hsa04728/hsa:9575%09red/hsa:406%09red
Primary bile acid biosynthesis	KEGG PATHWAY	hsa00120	1	17	4.97×10^{-03}	1.24×10^{-02}	1581	http://www.genome.jp/kegg-bin/show_pathway?hsa00120/hsa:1581%09red
Fat digestion and absorption	KEGG PATHWAY	hsa04975	1	41	1.16×10^{-02}	2.37×10^{-02}	19	http://www.genome.jp/kegg-bin/show_pathway?hsa04975/hsa:19%09red
ABC transporters	KEGG PATHWAY	hsa02010	1	45	1.27×10^{-02}	2.37×10^{-02}	19	http://www.genome.jp/kegg-bin/show_pathway?hsa02010/hsa:19%09red
Steroid hormone biosynthesis	KEGG PATHWAY	hsa00140	1	58	1.62×10^{-02}	2.70×10^{-02}	1581	http://www.genome.jp/kegg-bin/show_pathway?hsa00140/hsa:1581%09red
Bile secretion	KEGG PATHWAY	hsa04976	1	71	1.97×10^{-02}	2.96×10^{-02}	1581	http://www.genome.jp/kegg-bin/show_pathway?hsa04976/hsa:1581%09red
Insulin resistance	KEGG PATHWAY	hsa04931	1	109	3.00×10^{-02}	4.09×10^{-02}	10062	http://www.genome.jp/kegg-bin/show_pathway?hsa04931/hsa:10062%09red
Hepatitis C	KEGG PATHWAY	hsa05160	1	133	3.65×10^{-02}	4.56×10^{-02}	10062	http://www.genome.jp/kegg-bin/show_pathway?hsa05160/hsa:10062%09red
Non-alcoholic fatty liver disease	KEGG PATHWAY	hsa04932	1	151	4.13×10^{-02}	4.76×10^{-02}	10062	http://www.genome.jp/kegg-bin/show_pathway?hsa04932/hsa:10062%09red
Transcriptional misregulation in cancer	KEGG PATHWAY	hsa05202	1	180	4.89×10^{-02}	5.24×10^{-02}	8864	http://www.genome.jp/kegg-bin/show_pathway?hsa05202/hsa:8864%09red
Metabolic pathways	KEGG PATHWAY	hsa01100	1	1,243	2.95×10^{-01}	2.95×10^{-01}	1581	http://www.genome.jp/kegg-bin/show_pathway?hsa01100/hsa:1581%09red

Data from the KEGG pathway database. The statistical methods used were the hypergeometric and Fisher's exact tests. The Benjamini and Hochberg FDR correction method was applied. KEGG, Kyoto Encyclopedia of Genes and Genomes; FDR, false discovery rate.

peripheral clock systems are independent from the central clock system, the present study results suggested that renal injury lead to local circadian system disorder, which may have caused the impaired function of the core clock gene to affect the liver, subsequently disrupting lipid metabolism. In order to confirm the phenomenon observed in the present study, further studies are required.

In conclusion, the present study reported that NS rats exhibited dyslipidemia and circadian disorders of lipid metabolism. The results suggested that these changes involve the abnormal expression of hepatic core clock genes and downstream clock-controlled genes. Furthermore, the findings indicated that damage to the hepatic clock system is a potential molecular mechanism for disordered blood lipid circadian rhythm in the context of CKD. Such analyses offer a starting point for understanding the crosstalk between peripheral organs and peripheral clock systems. Further investigations into the prevention and treatment of CKD by resetting or repairing disturbed central or peripheral clock systems are required.

Acknowledgements

Not applicable.

Funding

The present study was supported by the National Natural Sciences Foundation of China (grant no. 81100545), The Beijing Municipal Science and Technology Commission (grant nos. D131100004713007 and D09050704310901), and The Peking Union Medical College Youth Fund (grant no. 3332016012).

Availability of data and materials

All data generated or analyzed during this study are included in this published article.

Authors' contributions

PC, RZ, LM, XwL, XmL and YQ contributed to the conception and design of this study. PC, RZ and LM performed the experiments. PC analyzed and interpretation of data. PC and YQ drafted the manuscript. All the authors read and gave final approval of the version to be published.

Ethics approval and consent to participate

The animal experimental procedures were approved by the Animal Ethics Committee of Peking Union Medical College Hospital (Beijing, China).

Patient consent for publication

Not applicable.

Competing interests

The authors declare that they have no competing interests.

References

1. Harper CR and Jacobson TA: Managing dyslipidemia in chronic kidney disease. J Am Coll Cardiol 51: 2375-2384, 2008.
2. Tsimihodimos V, Dounousi E and Siamopoulos KC: Dyslipidemia in chronic kidney disease: An approach to pathogenesis and treatment. Am J Nephrol 28: 958-973, 2008.
3. Zhao X, Cho H, Yu RT, Atkins AR, Downes M and Evans RM: Nuclear receptors rock around the clock. EMBO Rep 15: 518-528, 2014.
4. Zhang EE and Kay SA: Clocks not winding down: Unravelling circadian networks. Nat Rev Mol Cell Biol 11: 764-776, 2010.
5. Ungar F and Halberg F: Circadian rhythm in the in vitro response of mouse adrenal to adrenocorticotropic hormone. Science 137: 1058-1060, 1962.
6. Mure LS, Le HD, Benegiamo G, Chang MW, Rios L, Jillani N, Ngotho M, Kariuki T, Dkhissi-Benyahya O, Cooper HM and Panda S: Diurnal transcriptome atlas of a primate across major neural and peripheral tissues. Science 359: eaao0318, 2018.
7. Tokonami N, Mordasini D, Pradervand S, Centeno G, Jouffe C, Maillard M, Bonny O, Gachon F, Gomez RA, Sequeira-Lopez ML and Firsov D: Local renal circadian clocks control fluid-electrolyte homeostasis and BP. J Am Soc Nephrol 25: 1430-1439, 2014.
8. Reppert SM and Weaver DR: Coordination of circadian timing in mammals. Nature 418: 935-941, 2002.
9. Oosterman JE, Kalsbeek A, la Fleur SE and Belsham DD: Impact of nutrients on circadian rhythmicity. Am J Physiol Regul Integr Comp Physiol 308: R337-R350, 2015.
10. Wharfe MD, Mark PJ and Waddell BJ: Circadian variation in placental and hepatic clock genes in rat pregnancy. Endocrinology 152: 3552-3560, 2011.
11. Touitou Y, Smolensky MH and Portaluppi F: Ethics, standards, and procedures of animal and human chronobiology research. Chronobiol Int 23: 1083-1096, 2006.
12. Nguyen TT, Mattick JS, Yang Q, Orman MA, Ierapetritou MG, Berthiaume F and Androulakis IP: Bioinformatics analysis of transcriptional regulation of circadian genes in rat liver. BMC Bioinformatics 15: 83, 2014.
13. Wu T, ZhuGe F, Zhu Y, Wang N, Jiang Q, Fu H, Li Y and Fu Z: Effects of light on the circadian rhythm of diabetic rats under restricted feeding. J Physiol Biochem 70: 61-71, 2014.
14. Bertani T, Poggi A, Pozzoni R, Delaini F, Sacchi G, Thoua Y, Mecca G, Remuzzi G and Donati MB: Adriamycin-induced nephrotic syndrome in rats: Sequence of pathologic events. Lab Invest 46: 16-23, 1982.
15. Lu B, Li X and Ma R: Evaluation of the modified adriamycin induced nephrotic rats. Lab Anim Sci Admin 16: 5-9, 1999 (In Chinese).
16. Pereira Wde F, Brito-Melo GE, de Almeida CA, Moreira LL, Cordeiro CW, Carvalho TG, Mateo EC, Simões E and Silva AC: The experimental model of nephrotic syndrome induced by Doxorubicin in rodents: An update. Inflamm Res 64: 287-301, 2015.
17. Brainard GC, Richardson BA, King TS and Reiter RJ: The influence of different light spectra on the suppression of pineal melatonin content in the Syrian hamster. Brain Res 294: 333-339, 1984.
18. Trinder P and Webster D: Determination of HDL-cholesterol using 2,4,6-tribromo-3-hydroxybenzoic acid with a commercial CHOD-PAP reagent. Ann Clin Biochem 21: 430-433, 1984.
19. Friedewald WT, Levy RI and Fredrickson DS: Estimation of the concentration of low-density lipoprotein cholesterol in plasma, without use of the preparative ultracentrifuge. Clin Chem 18: 499-502, 1972.
20. Westgard JO and Poquette MA: Determination of serum albumin with the 'SMA 12-60' by a bromcresol green dye-binding method. Clin Chem 18: 647-653, 1972.
21. Fossati P, Prencipe L and Berti G: Enzymic creatinine assay: A new colorimetric method based on hydrogen peroxide measurement. Clin Chem 29: 1494-1496, 1983.
22. Neeley WE: Simple automated determination of serum or plasma glucose by a hexokinase-glucose-6-phosphate dehydrogenase method. Clin Chem 18: 509-515, 1972.
23. Livak KJ and Schmittgen TD: Analysis of relative gene expression data using real-time quantitative PCR and the 2(-Delta Delta C(T)) method. Methods 25: 402-408, 2001.
24. Szklarczyk D, Franceschini A, Kuhn M, Simonovic M, Roth A, Minguez P, Doerks T, Stark M, Muller J, Bork P, *et al*: The STRING database in 2011: Functional interaction networks of proteins, globally integrated and scored. Nucleic Acids Res 39: D561-D568, 2011.

25. Huang da W, Sherman BT and Lempicki RA: Bioinformatics enrichment tools: Paths toward the comprehensive functional analysis of large gene lists. Nucleic Acids Res 37: 1-13, 2009.
26. Shannon P, Markiel A, Ozier O, Baliga NS, Wang JT, Ramage D, Amin N, Schwikowski B and Ideker T: Cytoscape: A software environment for integrated models of biomolecular interaction networks. Genome Res 13: 2498-2504, 2003.
27. Walter W, Sánchez-Cabo F and Ricote M: GOplot: An R package for visually combining expression data with functional analysis. Bioinformatics 31: 2912-2914, 2015.
28. Paul T and Lemmer B: Disturbance of circadian rhythms in analgosedated intensive care unit patients with and without craniocerebral injury. Chronobiol Int 24: 45-61, 2007.
29. Palma-Rigo K, Baudrie V, Laude D, Petrel C, Clauser E and Elghozi JL: Cardiovascular rhythms and cardiac baroreflex sensitivity in AT(1A) receptor gain-of-function mutant mice. Chronobiol Int 27: 128-137, 2010.
30. Lee VW and Harris DC: Adriamycin nephropathy: A model of focal segmental glomerulosclerosis. Nephrology (Carlton) 16: 30-38, 2011.
31. Mamdani M, Williamson V, McMichael GO, Blevins T, Aliev F, Adkins A, Hack L, Bigdeli T, van der Vaart AD, Web BT, *et al*: Integrating mRNA and miRNA weighted gene co-expression networks with eQTLs in the nucleus accumbens of subjects with alcohol dependence. PLoS One 10: e0137671, 2015.
32. Szklarczyk D, Morris JH, Cook H, Kuhn M, Wyder S, Simonovic M, Santos A, Doncheva NT, Roth A, Bork P, *et al*: The STRING database in 2017: Quality-controlled protein-protein association networks, made broadly accessible. Nucleic Acids Res 45: D362-D368, 2017.
33. Szklarczyk D, Franceschini A, Wyder S, Forslund K, Heller D, Huerta-Cepas J, Simonovic M, Roth A, Santos A, Tsafou KP, *et al*: STRING v10: Protein-protein interaction networks, integrated over the tree of life. Nucleic Acids Res 43 (Database Issue): D447-D452, 2015.
34. Huang da W, Sherman BT and Lempicki RA: Systematic and integrative analysis of large gene lists using DAVID bioinformatics resources. Nat Protoc 4: 44-57, 2009.
35. Feng G, Shaw P, Rosen ST, Lin SM and Kibbe WA: Using the bioconductor GeneAnswers package to interpret gene lists. Methods Mol Biol 802: 101-112, 2012.
36. Wahl P, Ducasa GM and Fornoni A: Systemic and renal lipids in kidney disease development and progression. Am J Physiol Renal Physiol 310: F433-F445, 2016.
37. Rogacev KS, Pinsdorf T, Weingärtner O, Gerhart MK, Welzel E, van Bentum K, Popp J, Menzner A, Fliser D, Lütjohann D and Heine GH: Cholesterol synthesis, cholesterol absorption, and mortality in hemodialysis patients. Clin J Am Soc Nephrol 7: 943-948, 2012.
38. Kaysen GA: Nonrenal complications of the nephrotic syndrome. Ann Rev Med 45: 201-210, 1994.
39. Schalk BW, Visser M, Deeg DJ and Bouter LM: Lower levels of serum albumin and total cholesterol and future decline in functional performance in older persons: The Longitudinal Aging Study Amsterdam. AGE Ageing 33: 266-272, 2004.
40. Lamia KA, Storch KF and Weitz CJ: Physiological significance of a peripheral tissue circadian clock. Proc Natl Acad Sci USA 105: 15172-15177, 2008.
41. Richards J, All S, Skopis G, Cheng KY, Compton B, Srialluri N, Stow L, Jeffers LA and Gumz ML: Opposing actions of Per1 and Cry2 in the regulation of Per1 target gene expression in the liver and kidney. Am J Physiol Regul Integr Comp Physiol 305: R735-R747, 2013.
42. Chua EC, Shui G, Lee IT, Lau P, Tan LC, Yeo SC, Lam BD, Bulchand S, Summers SA, Puvanendran K, *et al*: Extensive diversity in circadian regulation of plasma lipids and evidence for different circadian metabolic phenotypes in humans. Proc Natl Acad Sci USA 110: 14468-14473, 2013.
43. Nikolaeva S, Pradervand S, Centeno G, Zavadova V, Tokonami N, Maillard M, Bonny O and Firsov D: The circadian clock modulates renal sodium handling. J Am Soc Nephrol 23: 1019-1026, 2012.
44. Hou XW, Jiang Y, Wang LF, Xu HY, Lin HM, He XY, He JJ and Zhang S: Protective role of granulocyte colony-stimulating factor against adriamycin induced cardiac, renal and hepatic toxicities. Toxicol Lett 187: 40-44, 2009.
45. Bertani T, Cutillo F, Zoja C, Broggini M and Remuzzi G: Tubulo-interstitial lesions mediate renal damage in adriamycin glomerulopathy. Kidney Int 30: 488-496, 1986.
46. Pippin JW, Brinkkoetter PT, Cormack-Aboud FC, Durvasula RV, Hauser PV, Kowalewska J, Krofft RD, Logar CM, Marshall CB, Ohse T and Shankland SJ: Inducible rodent models of acquired podocyte diseases. Am J Physiol Renal Physiol 296: F213-F229, 2009.
47. Rudic RD, McNamara P, Curtis AM, Boston RC, Panda S, Hogenesch JB and Fitzgerald GA: BMAL1 and CLOCK, two essential components of the circadian clock, are involved in glucose homeostasis. PLoS Biol 2: e377, 2004.
48. Rivera-Coll A, Fuentes-Arderiu X and Diez-Noguera A: Circadian rhythmic variations in serum concentrations of clinically important lipids. Clin Chem 40: 1549-1553, 1994.
49. Van den Berg R, Noordam R, Kooijman S, Jansen SWM, Akintola AA, Slagboom PE, Pijl H, Rensen PCN, Biermasz NR and van Heemst D: Familial longevity is characterized by high circadian rhythmicity of serum cholesterol in healthy elderly individuals. Aging cell 16: 237-243, 2017.
50. Fonken LK, Aubrecht TG, Meléndez-Fernández OH, Weil ZM and Nelson RJ: Dim light at night disrupts molecular circadian rhythms and increases body weight. J Biol Rhythms 28: 262-271, 2013.
51. Baeza-Raja B, Eckel-Mahan K, Zhang L, Vagena E, Tsigelny IF, Sassone-Corsi P, Ptácek LJ and Akassoglou K: p75 neurotrophin receptor is a clock gene that regulates oscillatory components of circadian and metabolic networks. J Neurosci 33: 10221-10234, 2013.
52. Honma S, Kawamoto T, Takagi Y, Fujimoto K, Sato F, Noshiro M, Kato Y and Honma K: Dec1 and Dec2 are regulators of the mammalian molecular clock. Nature 419: 841-844, 2002.
53. Kato Y, Kawamoto T, Fujimoto K and Noshiro M: DEC1/STRA13/SHARP2 and DEC2/SHARP1 coordinate physiological processes, including circadian rhythms in response to environmental stimuli. Curr Top Dev Biol 110: 339-372, 2014.
54. Edwards PA, Kast HR and Anisfeld AM: BAREing it all: The adoption of LXR and FXR and their roles in lipid homeostasis. J Lipid Res 43: 2-12, 2002.
55. Bodzioch M, Orsó E, Klucken J, Langmann T, Böttcher A, Diederich W, Drobnik W, Barlage S, Büchler C, Porsch-Ozcürümez M, *et al*: The gene encoding ATP-binding cassette transporter 1 is mutated in Tangier disease. Nat Genet 22: 347-351, 1999.
56. Bossi P, Bergamini C, Siano M, Cossu Rocca M, Sponghini AP, Favales F, Giannoccaro M, Marchesi E, Cortelazzi B, Perrone F, *et al*: Functional genomics uncover the biology behind the responsiveness of head and neck squamous cell cancer patients to cetuximab. Clin Cancer Res 22: 3961-3970, 2016.
57. D'Amato G, Luxán G, del Monte-Nieto G, Martínez-Poveda B, Torroja C, Walter W, Bochter MS, Benedito R, Cole S, Martinez F, *et al*: Sequential Notch activation regulates ventricular chamber development. Nat Cell Biol 18: 7-20, 2016.
58. Boerwinkle E, Menzel HJ, Kraft HG and Utermann G: Genetics of the quantitative Lp(a) lipoprotein trait. III. Contribution of Lp(a) glycoprotein phenotypes to normal lipid variation. Hum Genet 82: 73-78, 1989.